A Multiparameter Moment Matching Model Reduction Approach for Generating Geometrically Parameterized Interconnect Performance Models

Luca Daniel, Ong Chin Siong, Low Sok Chay, Kwok Hong Lee, and Jacob White.

***Abstract*— In this paper we describe an approach for generating accurate geometrically-parameterized integrated-circuit interconnect models that are efficient enough for use in interconnect synthesis. The model generation approach presented is automatic, and is based on a multi-parameter moment matching model-reduction algorithm. A moment matching theorem proof for the algorithm is derived, as well as a complexity analysis for the model order growth. The effectiveness of the technique is tested using a capacitance extraction example, where the plate spacing is considered as the geometric parameter, and a multi-line bus example, where both wire spacing and wire width are considered as geometric parameters. Experimental results demonstrate that the generated models accurately predict capacitance values for the capacitor example, and both delay and cross-talk effects over a reasonably wide range of spacing and width variation for the multi-line bus example.**

***Index terms* - Interconnect synthesis, modeling, model order reduction, parameterized model order reduction.**

I. Introduction

Developers of routing tools for mixed signal applications could make productive use of more accurate performance models for interconnect, but the cost of extracting even a modestly accurate model for a candidate route is far beyond the computational budget of the inner loop of a router. If it were possible to extract geometrically parameterized, but inexpensive to evaluate, models for the interconnect performance, then such models could be used for detailed interconnect synthesis in performance critical digital or analog applications.

The idea of generating parameterized reduced-order interconnect models is not new, recent approaches have been developed that focus on statistical performance evaluation [1], [2] and clock skew minimization [3]. However, our target application, interconnect synthesis, requires parameterized models valid over a wide geometric range. Generating such parameterized models is made difficult by the fact that even though the electrical behavior of interconnect can be modeled by a linear time-invariant dynamical system, that system typically depends nonlinearly on geometric parameters.

One recently developed technique for generating geometrically parameterized models of physical systems assumed a linear dependence on the parameter, and was applied to reducing a discretized linear partial differential equation [4]. The approach used closely paralleled the techniques used for dynamical system model reduction, an unsurprising fact given that if the parameter dependence is linear, the generated parameterized system of equations is structurally identical to a Laplace transform description of a linear time-invariant dynamical system, though the frequency variable is in the place of the geometric parameter.

The observation that geometric parameters and frequency variables are interchangeable, at least when the dependence of the geometric variation is linear, suggests that the parameterized reduction problem could be formulated so as to make use of extensions to the projection-subspace based moment matching methods that have proved so effective in interconnect modeling [5], [6], [7], [8], [9], [10], [11], [12], [13]. In this paper we develop approaches for generating parameterized interconnect models exploiting just such a connection. We start in the next section by examining the single geometric parameter case, and treat the case when the variation with respect to the geometric parameter is nonlinear. In Section III, we apply the single parameter approaches to the problem of automatically extracting parameterized models for interconnect capacitances from integral equation based capacitance extraction techniques. In Section IV we present a more general problem formulation for an arbitrary number of parameters. In Section V we extend the two-parameter moment matching model reduction technique in [14], introducing a moment matching model reduction algorithm for an arbitrary number of parameters. In the same section we also derive a rigorous proof for the moment matching properties of our algorithm. In Section VI we analyze the complexity of the algorithm in terms of model order growth as a function of the number of parameters, and the cost of the model construction as a function of the size of the original system. In Sections VII we demonstrate the practical effectiveness of the method on a wire-spacing parameterized multi-line bus example, and consider both delay and cross-talk effects. In Section VIII we use the generalized multi-parameter model reduction approach to re-examine the multi-line bus example, but now allow both wire width and wire spacing together with frequency to be parameters. Finally, conclusions are given in Section IX.

II. The Single Parameter Case

In this section we consider the single parameter case, and in the next section we will use the resulting algorithm to

Luca Daniel (617-253-2631 luca@mit.edu), and Jacob White (617-253-2543 white@mit.edu), are with the Department of Electrical Engineering and Computer Science, Massachusetts Institute of Technology, 77 Massachusetts Ave 36-807, 02139 Cambridge, MA.

Ong Chin Siong, Low Sok Chay, and Kwok Hong Lee are with the National University of Singapore.

generate parameterized formulas for interconnect coupling capacitances. In examining this simpler case, we hope to clarify some of the issues that will arise in multiparameter reduction and better establish the connections between our approach with work by others.

To begin, consider a single parameter linear system

$$\begin{aligned} E(s)x &= Bu \\ y &= Cx \end{aligned} \tag{1}$$

where s is the parameter; x is the vector of "states", a term we use loosely because s is not necessarily the Laplace frequency parameter, and the system in (1) is a "dynamical system in state space form" only when s is the Laplace frequency parameter. Vectors u and y are t-dimensional input and output vectors; $E(s)$ is an $n \times n$ matrix; and B and C are $n \times t$ and $t \times n$ matrices which define how the inputs and outputs relate to the state vector x.

For many interconnect problems, the number of inputs and outputs, t, is typically much smaller than n, the number of states needed to accurately represent the electrical behavior of the interconnect. In order to generate a representation of the input-output behavior given by (1) using many fewer states, a projection approach is commonly used [8]. In the projection approach, one first constructs an $n \times q$ projection matrix V where $q \ll n$, and then one generates the reduced model from the original system using congruence transformations [7]. Specifically, the reduced system is given by

$$\begin{aligned} [V^T E(s) V]\hat{x} &= V^T B u \\ y &= CV\hat{x} \end{aligned} \tag{2}$$

where the reduced state vector $\hat{x}$ is of dimension q and is representing the projection of the large original state vector $x \approx V\hat{x}$. Note, the columns of V are typically chosen in such a way that the final response of the reduced system matches q terms in the Taylor series expansion in s of the original response regardless if s is a Laplace frequency parameter or instead some other kind of geometrical parameter.

The reduced order system given in (2) is not really an efficient reduced model, as explicit evaluation of $V^T E(s) V$ requires order n^2 operations is $E(s)$ is dense and nq operations if $E(s)$ is sparse. To generate a reduced model that can be more efficiently evaluated, consider using polynomial interpolation or a Taylor series expansion to generate a representation of $E(s)$ that can be expressed as a power series,

$$E(s) = \sum_{m=0}^{\infty} s^m E_m. \tag{3}$$

There are several approaches for constructing a reduced-order model given the $E(s)$ in (3). If the power series is truncated to order p, it is possible to transform the power series reduction problem to a p-parameter reduction problem, with only a linear dependence on the newly introduced parameters $s_m = s^m$, $m = 1, ..., p$, as in

$$E(s) \approx E_0 + s_1 E_1 + s_2 E_2 + ... + s_p E_p \tag{4}$$

After this transformation, the multiparameter algorithms which will be described in subsequent Section V can be used directly, though the dimension of the resulting reduced model may be unnecessarily high.

A more efficient reduction approach can be derived by converting (1) to a linear single-parameter reduction problem by introducing fictitious states [15]. The resulting representation of $E(s)$ is linearly dependent on s and is given by

$$\left\{ \begin{bmatrix} E_0 & & & \\ & I & & \\ & & I & \\ & & & \ddots \end{bmatrix} - s \begin{bmatrix} -E_1 & -E_2 & -E_3 & \cdots \\ I & & & \\ & I & & \\ & & \ddots & \end{bmatrix} \right\} \begin{bmatrix} x \\ x_1 \\ x_2 \\ \vdots \end{bmatrix} = \begin{bmatrix} B \\ 0 \\ 0 \\ \vdots \end{bmatrix} u \tag{5}$$

where the fictitious states, denoted x_i, satisfy the relation

$$x_1 = sx \quad x_2 = sx_1 \quad x_3 = sx_2 \quad \ldots$$

Examination of (5) yields a series expansion for x in terms of the parameter s. That is,

$$x = \sum_{m=0}^{\infty} s^m F^m, \tag{6}$$

where

$$F^m = -\sum_{k=0}^{m-1} E_0^{-1} E_{m-k} F^k, \quad m > 0 \tag{7}$$

and

$$F^0 = E_0^{-1} B. \tag{8}$$

The projection matrix used to generate a q^{th} reduced-order model is then given by

$$\text{colspan}(V) \supseteq \text{span}\{F^0, F^1, ..., F^{q-1}\}.$$

and the reduced model is

$$\begin{aligned} \left(\sum_{m=0}^{p} V^T E_m V s^m \right) \hat{x} &= V^T B u \\ y &= CV\hat{x}. \end{aligned} \tag{9}$$

III. Parameterized Capacitance Extraction

In this section we use the single parameter model reduction strategy described above to generate parameterized models for interconnect self and coupling capacitances. We start with a brief description of the capacitance extraction problem, and then describe how we made use of the model reduction.

A. Computing Capacitances

Consider the three conductors example in Fig. 1, in which we are interested in determining the relation between the coupling capacitances and the conductor separation distances. The matrix of self and coupling capacitances is usually computed by solving an integral equation for the conductor surface charges, and then integrating those charges to determine conductor capacitances. In particular, the surface charge density, σ, must satisfy the first-kind integral equation

$$\psi(r) = \int_{surfaces} \sigma(r') \frac{1}{4\pi\varepsilon_0 ||r - r'||} da', \tag{10}$$

where r and r' are positions on the conductor surfaces, $\psi(r)$ is the known conductor surface potential, da' is the incremental conductor surface area, and $||r||$ is the usual Euclidean length of r.

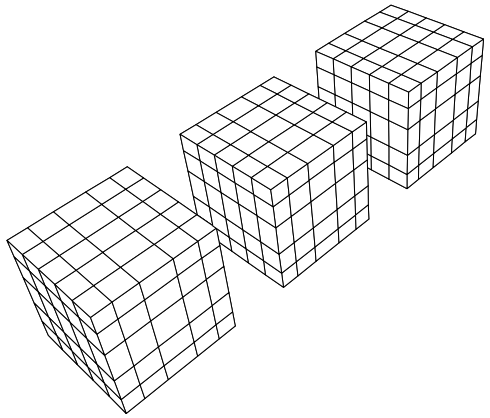

Fig. 1. Three conductors example for capacitance extraction. Conductors are $1m \times 1m \times 1m$. Nominal gap is $0.5m$. The discretization of the surface into small panels is also shown.

A standard approach to numerically solving (10) for σ is to use a piece-wise constant collocation scheme. In such schemes, the conductor surfaces are divided up into n small panels, and σ is assumed constant on each panel, thus generating a piecewise constant approximation to σ. The n panel charges can then be determined by insisting that the approximation to σ generates the correct potential at n test points located at the centroids of the n panels. This constraint on the panel charges can be represented as a linear system of equations

$$Ex = b \tag{11}$$

where E is the dense matrix which relates unknown panel charges to known panel potentials, x is the vector of panel charges, $b \in \mathbf{R}^n$ is the vector of known panel centroid potentials, and

$$E_{ij} = \frac{1}{a_j} \int_{panel_j} \frac{1}{4\pi\varepsilon_0 ||r_i - r'||} da', \tag{12}$$

where r_i is the centroid of the i-th panel and a_j is the area of the j-th panel.

For the three conductor example shown in Fig. 1, there are a total of six coupling capacitances and three self capacitances. To determine these capacitance values, one can solve (11) three times, with three different b vectors. Specifically, the three different b vectors are used to set a nonzero voltage on only one conductor at a time. Weighted combinations of the three computed vectors of panel charges, x, then yield the self and coupling capacitances. Altering the spacing between the three conductors will change the separation distances between pairs of panels and centroids that reside on different conductors. As is clear from the formula for the potential coefficients, equation (12), the E_{ij}'s depend nonlinearly on the panel separation distances, and therefore the matrix E depends nonlinearly on conductor separation distances.

B. Approximating The Potential Coefficient Matrix

In order to apply the above techniques for model reduction to the capacitance extraction problem, it is first necessary to generate a polynomial approximation for the variations in the potential coefficient matrix, E, caused by variations in separation distance w. For the three conductors example in Fig. 1, we used both a Taylor series and Chebyshev polynomial interpolation approaches to generate a quadratic approximation of the form

$$E(w) \approx E_0 + wE_1 + w^2E_2.$$

where note that E_0, E_1 and E_2 are $n \times n$ matrices. After the polynomial coefficients are obtained, they can be used in the recursion formula (7) to generate V, which can in turn be used to obtain a reduced system. Hence,

$$\begin{aligned} &E(w)x = b \\ &\qquad \Downarrow \text{Taylor or Chebyshev approximation} \\ &(E_0 + wE_1 + w^2E_2)\hat{x} = b \\ &\qquad \Downarrow \text{Model Order Reduction} \\ &\qquad \text{through recursion formula} \\ &V^T(E_0 + wE_1 + w^2E_2)V\hat{x} = V^Tb \end{aligned}$$

Example capacitance results for the three conductors example are shown in Fig. 2 and 3. The conductors were discretized into approximately 600 panels, (12) was used to compute the $E(w)$ matrix, and (11) was solved to determine normalized self and coupling capacitances for the conductors. In addition, $E(w)$ was fit with a quadratic expansion in w using a Taylor series and a Chebyshev expansion, and then these expanded matrices were reduced, as described above.

In Fig. 2 the self and coupling capacitances computed using the exact $E(w)$ are compared to those produced using quadratic models generated using the Taylor and Chebyshev approximations (no model reduction was applied). As is clear from the figure, the quadratic approximations fit reasonably well from one fifth of the nominal gap spacing to nearly twice the gap spacing. Both the Taylor and Chebyshev methods become inaccurate for very small conductor separations, and the Chebyshev method is more accurate for large separations, being indistinguishable from the exact $E(w)$ solution at 1.8 times the nominal spacing, at least for the self and largest coupling capacitance. Note that the capacitance coupling for the first and third conductor is an order of magnitude smaller than the self and nearby coupling capacitances, but is still approximated reasonably accurately.

In order to examine the impact on accuracy of the model reduction, the three 600×600 matrices generated by the quadratic Chebyshev expansion were reduced to 5×5 and 7×7 matrices using the congruence projection model reduction described above. Once the reduced matrices are calculated, evaluating the self and coupling capacitances for a new value of w is just a matter of a few very simple additions and factorizations operations on matrices of order 5×5 or 7×7. As shown in Fig. 3, the capacitances computed using the original 600×600 Chebyshev matrices are indistinguishable from those generated by the reduced models for the self and nearby coupling capacitances. In addition, the reduced model results are still reasonable for the much smaller distance coupling capacitance.

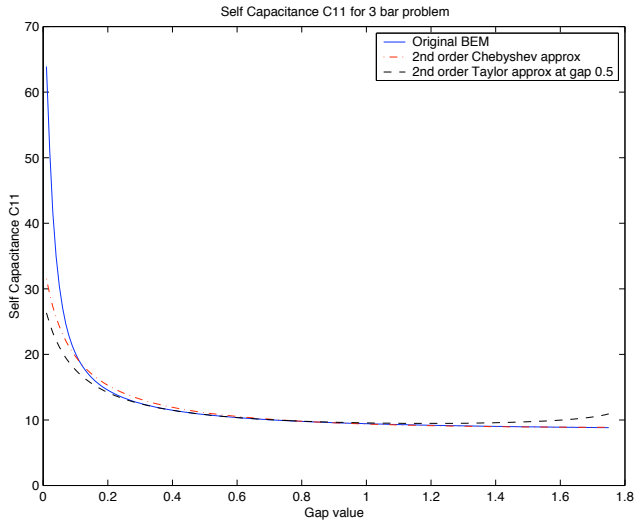

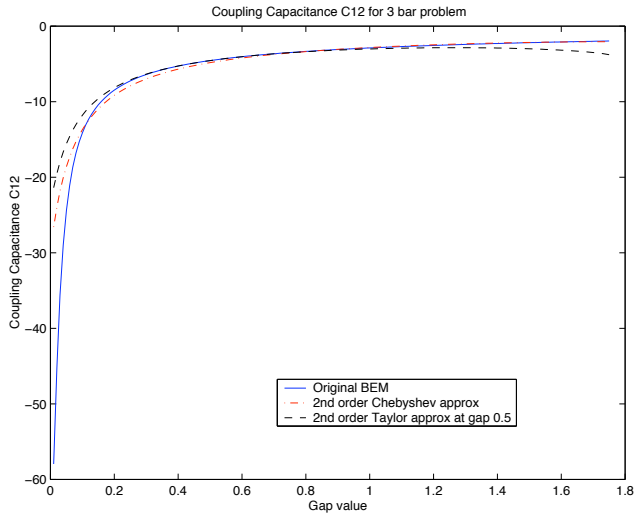

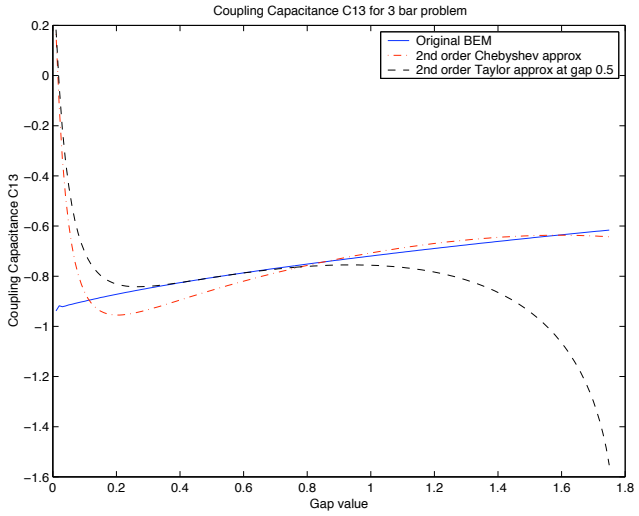

Fig. 2. This figure illustrates the error introduced by the first step of our procedure: in this example an approximation using 2nd order Taylor or Chebyshev Polynomials. Taylor is better locally around its expansion point (gap = 0.5m), while Chebyshev is better on a wider range of values, yet still finite (e.g. see lower plot). No model order reduction technique has been applied at this stage. Capacitances values should be scaled by 10pF, gap is in *m*.

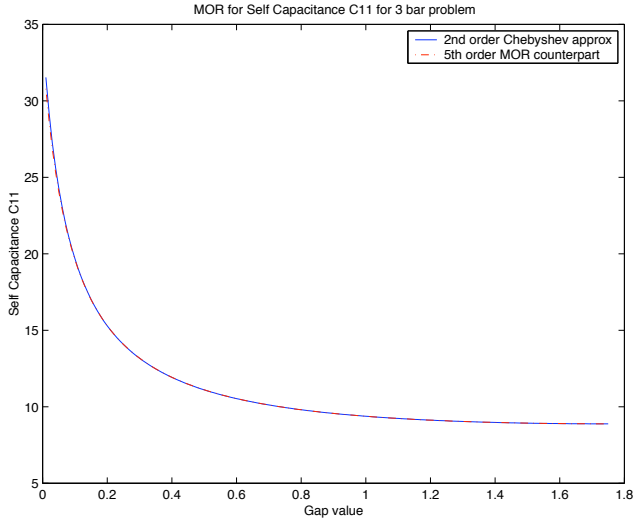

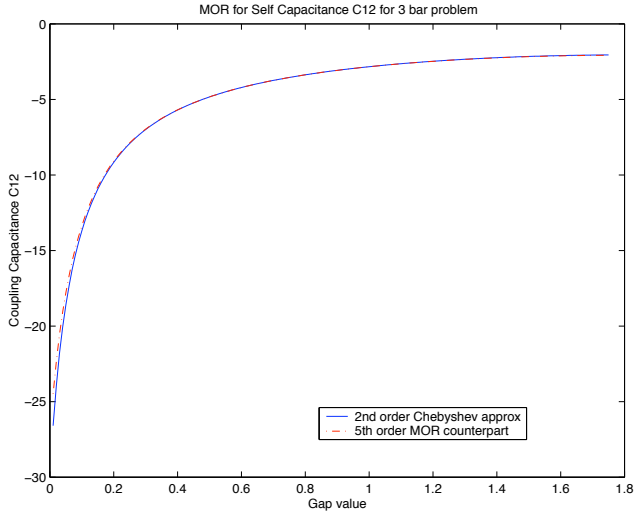

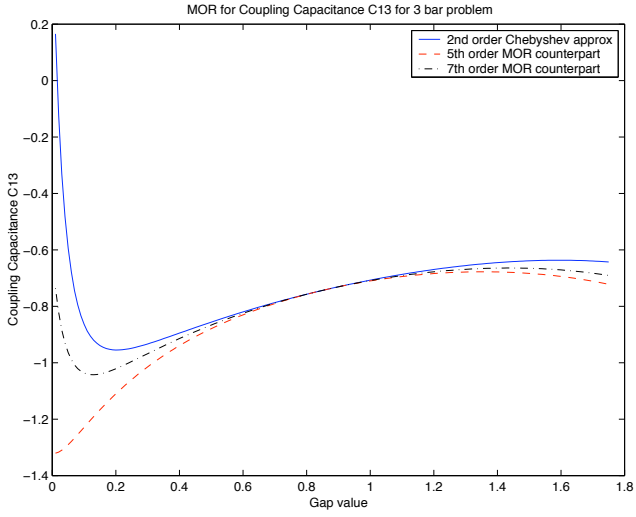

Fig. 3. This figure illustrates the additional error introduced by the actual model order reduction step (second step). The reference for the comparison in this figure is the result of the first step: the 2nd order Chebyshev approximation. The reduction step produces a good fit around the expansion point. However the model is valid only for a finite range of values of the parameter. Higher orders are shown to yield higher accuracies and wider ranges. Capacitance values should be scaled by 10pF, gap is in *m*.

IV. A MORE GENERAL PROBLEM FORMULATION

When modeling long interconnect wires, it is usually insufficiently accurate to use a simple lumped capacitor model. Instead, the long wires are usually modeled using a distribution of resistors and capacitors, and sometimes even inductors. Even if there is only one geometric parameter of interest, such interconnect examples still generate a multiparameter reduction problem, with frequency being the second parameter.

In order to derive an approach for the multiparameter problem, consider the following parameterized state space system model:

$$\begin{aligned} E(s_1,\ldots,s_\mu)x &= Bu \\ y &= Cx, \end{aligned} \tag{13}$$

where $s_1,\ldots,s_\mu$ are μ parameters, x is the state of the system, $E(s_1,\ldots,s_\mu) \in \mathbf{R}^{n\times n}$ is the system descriptor matrix, B is a matrix relating the inputs u to the state x, and C is a matrix relating the state to the outputs y.

In general the descriptor matrix $E(s_1,\ldots,s_\mu)$ could have a complicated and non-linear dependence on the parameters $s_1,\ldots,s_\mu$. As a first step of our approach we capture this dependence by means of a power series in the parameters $s_1,\ldots,s_\mu$:

$$E(s_1,\ldots,s_\mu) = E_0 + \sum_i s_i E_i + \sum_{h,k} s_h s_k E_{h,k} + \sum_{h,k,j} s_h s_k s_j E_{h,k,j} + \ldots \tag{14}$$

One of the easiest ways to produce such a power series representation is to truncate the μ-variables Taylor series expansion shown in (15), where $\bar{s}_1,\ldots,\bar{s}_\mu$ are the expansion points. In a practical implementation, one could for instance choose the expansion points to coincide with the "nominal values" for each of the parameters. Also, in practical implementations one could be more interested in working explicitly with variables that represent relative variations $\Delta s_i/\bar{s}_i$ of the actual parameters around the expansion points, rather than working with absolute variations Δs_i. Finally, as an alternative to using a μ-variables Taylor series expansion, it is also possible to generate the power series representation using instead polynomial interpolation to a set of data points.

Given the power series representation in (14), a reduced order model can then be generated by using a congruence transformation on the power series representation, as in (16), where $V \in \mathbf{R}^{n\times q}$, and the size q of the reduced order system matrices is typically much smaller than the size n of the original system matrices.

In order to calculate the column span of the projection matrix V, it is convenient to use the power series (14) to rewrite system (13) as in (17), so that x is given by (18).

V. P PARAMETER MODEL ORDER REDUCTION

One simple way to construct the columns of the projection matrix V for the reduced order model in (16) is to identify a new set parameters $\tilde{s}_i$ and matrices $\tilde{E}_i$

$$\tilde{E}_i = \begin{cases} E_i & i=0,\ldots,\mu \\ E_{h,k} & h=1,\ldots,\mu;\ k=1,\ldots,\mu \\ E_{h,k,j} & h=1,\ldots,\mu;\ k=1,\ldots,\mu\ j=1,\ldots,\mu \\ \cdots & \end{cases}$$

$$\tilde{s}_i = \begin{cases} s_i & i=1,\ldots,\mu \\ s_h s_k & h=1,\ldots,\mu;\ k=1,\ldots,\mu \\ s_h s_k s_j & h=1,\ldots,\mu;\ k=1,\ldots,\mu\ j=1,\ldots,\mu \\ \cdots & \end{cases}$$

so that one can re-write the parameterized system in (13) as a linearly parameterized model

$$\begin{aligned} [\tilde{E}_0 + \tilde{s}_1\tilde{E}_1 + \cdots + \tilde{s}_p\tilde{E}_p]x &= Bu \\ y &= Cx. \end{aligned} \tag{19}$$

In the special case where the power series is constructed using a Taylor series expansion

$$\tilde{E}_0 = E(\bar{s}_1,\ldots,\bar{s}_p) \tag{20}$$

$$\tilde{E}_i = \begin{cases} \left[\bar{s}_i \frac{\partial E}{\partial s_i}(\bar{s}_1,\ldots,\bar{s}_p)\right] & i=1,\ldots,\mu \\ \left[\bar{s}_h\bar{s}_k \frac{\partial^2 E}{\partial s_h \partial s_k}(\bar{s}_1,\ldots,\bar{s}_p)\right] & h=1,\ldots,\mu;\ k=1,\ldots,\mu \\ \cdots & \end{cases}$$

$$\tilde{s}_i = \begin{cases} \left(\frac{\Delta s_i}{\bar{s}_i}\right) & i=1,\ldots,\mu \\ \left(\frac{\Delta s_h}{\bar{s}_h}\right)\left(\frac{\Delta s_k}{\bar{s}_k}\right) & h=1,\ldots,\mu;\ k=1,\ldots,\mu \\ \cdots & \end{cases} \tag{21}$$

In this simplified setting the reduced model is now

$$\begin{aligned} [V^T\tilde{E}_0V + \tilde{s}_1V^T\tilde{E}_1V + \cdots + \tilde{s}_pV^T\tilde{E}_pV]\hat{x} &= V^TBu \\ y &= CV\hat{x}, \end{aligned} \tag{22}$$

and once again, in order to calculate the column span of the projection matrix V it is convenient to write the system (19) as

$$\begin{aligned} [I - (\tilde{s}_1M_1 + \cdots + \tilde{s}_pM_p)]x &= B_Mu \\ y &= Cx, \end{aligned}$$

where

$$\begin{aligned} M_i &= -\tilde{E}_0^{-1}\tilde{E}_i \quad \text{for} \quad i=1,2,\ldots,p \\ B_M &= \tilde{E}_0^{-1}B. \end{aligned}$$

Hence x is given by (23).

Lemma 1: The coefficients $F^m_{k_2,\ldots,k_p}(M_1,\ldots,M_p)$ of the series in (23) can be calculated using (24).

The proof can be found in Appendix A. For a single input system, $B_M = b_M = \tilde{E}_0^{-1}b \in \mathbf{R}^{n\times 1}$, and the columns of V can be constructed to span the Krylov subspace (25), or equivalently (26).

The following lemmas are useful to prove the main moment matching theorem for parameterized model order reduction.

Lemma 2: If V is an orthonormal matrix $V \in \mathbf{R}^{n\times q}, V^TV = I_q \in \mathbf{R}^{q\times q}$, and z is any vector in the column span of the matrix V, $z \in \text{colspan}(V)$, then $VV^Tz = z$.

Note that "in general" $VV^T \neq I_n \in \mathbf{R}^{n\times n}$.

$$E(s_1,\ldots,s_\mu) = E(\bar{s}_1,\ldots,\bar{s}_\mu) + \sum_i \left(\frac{\Delta s_i}{\bar{s}_i}\right)\left[\bar{s}_i \frac{\partial E}{\partial s_i}(\bar{s}_1,\ldots,\bar{s}_\mu)\right] + \sum_{h,k}\left(\frac{\Delta s_h}{\bar{s}_h}\right)\left(\frac{\Delta s_k}{\bar{s}_k}\right)\left[\bar{s}_h\bar{s}_k \frac{\partial^2 E}{\partial s_h \partial s_k}(\bar{s}_1,\ldots,\bar{s}_\mu)\right] + \ldots \quad (15)$$

$$\left[V^T E_0 V + \sum_i s_i V^T E_i V + \sum_{h,k} s_h s_k V^T E_{h,k} V + \sum_{h,k,j} s_h s_k s_j V^T E_{h,k,j} V + \ldots\right] x = V^T B u, \qquad y = CVx \quad (16)$$

$$\left\{I - \left[\sum_i s_i(-E_0^{-1})E_i + \sum_{h,k} s_h s_k (-E_0^{-1})E_{h,k} + \sum_{h,k,j} s_h s_k s_j (-E_0^{-1})E_{h,k,j} + \ldots\right]\right\} x = E_0^{-1} B u \quad (17)$$

$$\begin{aligned} x &= \left\{I - \left[\sum_i s_i(-E_0^{-1})E_i + \sum_{h,k} s_h s_k (-E_0^{-1})E_{h,k} + \sum_{h,k,j} s_h s_k s_j (-E_0^{-1})E_{h,k,j} + \ldots\right]\right\}^{-1} E_0^{-1} B u \quad (18)\\ &= \sum_{m=0}^{\infty}\left[\sum_i s_i(-E_0^{-1})E_i + \sum_{h,k} s_h s_k (-E_0^{-1})E_{h,k} + \sum_{h,k,j} s_h s_k s_j (-E_0^{-1})E_{h,k,j} + \ldots\right]^m E_0^{-1} B u \end{aligned}$$

Lemma 3: If V is an orthonormal matrix $V \in \mathbf{R}^{n\times q}, V^T V = I_q$, and z is a vector such that $\tilde{E}_0^{-1} z \in \text{colspan}(V)$, then $(V^T \tilde{E}_0 V)^{-1} V^T z = V^T \tilde{E}_0^{-1} z$.

Lemma 4: If $F^m_{k_2,\ldots,k_p}(M_1,\ldots,M_p)$ is a matrix constructed as in (24), and $V \in \mathbf{R}^{n\times q}$ is an orthonormal matrix constructed such that (26) holds, then (27) holds for $m = 0,1,\ldots,m_q$.

Theorem 1: ***[Parameterized Model Order Reduction Moment Matching Theorem]. The first q moments (corresponding to the first m_q orders of derivatives in each parameter) of the transfer function for the reduced order model (22) constructed using the q columns of the orthonormal projection matrix $V \in \mathbf{R}^{n\times q}$ in (26) match the first q moments (corresponding to the first m_q orders of derivatives in each parameter) of the transfer function of the original system (19).***

Proofs for Lemma 2, 3, 4, and for Theorem 1 are given in Appendices B, C, D, and E respectively. Note that the development follows closely the two-parameter approach given in[14]. Extension of the parameterized model order reduction moment matching theorem to multi-input systems is straight forward. For a t-input system the columns of V can be constructed to span the Krylov subspaces produced by all the columns $[b_M]_j$ of B_M as shown in (28).

VI. Order Growth and Computational Complexity Analysis

Lemma 5: If p is the total number of parameters and m_q is the largest order of derivative that will be matched with respect to any parameter, then the order q of the parameterized reduced system is

$$q = O\left(\frac{p^{m_q}}{m_q^{m_q-\frac{1}{2}}}\right)$$

One way to improve accuracy is to increase m_q. Unfortunately, with large m_q the order of the produced model might quickly become impractical. When $m_q = 1$, the order of the produced model scales linearly with the number of parameters and a large number of parameters can be handled. In some applications the accuracy given by matching a single derivative per parameter can be good enough. In particular, we recall that many of the examples presented in this paper are obtained using $m_q = 1$ and show good accuracy. Using $m_q = 2$ improves the accuracy but generates a larger system. For example, with $m_q = 2$ the order of the produced parameterized model is

$$q = f_{0,p} + f_{1,p} + f_{2,p} = 1 + p + \frac{p(p+1)}{2} = \frac{p^2+3p+2}{2}$$

which implies that a 66^{th} order model will be generated from a problem with $p = 10$ parameters. For larger values of m_q, impractically large models will be generated even for a small number of parameters p.

In terms of computational cost, it is important to make a distinction between the cost of "constructing" the model and the cost of "evaluating" the model. The models constructed by our procedure are extremely small compared to the original systems, therefore their evaluation cost is also small compared to the construction cost. In particular, when constructing the model, most of the cost is in constructing each of the q columns of matrix V. In particular, generating vectors F^m defined in (24), is the most expensive operation, given that it involves iterative large and dense matrix solves for A_{-1} in M_j, and several other large and dense matrix-vector multiplications. In order to make the cost of model computation practical one can use Krylov subspace iterative methods combined with "fast-methods" [16], [17], [18], [19], [20] for the required matrix-vector products. Exploiting such well developed techniques we need to perform $O(n\log(n))$ operations for each column of V. Hence the total construction cost is $O(qn)$, where q is typically on the order of few hundreds, and n can be as large as hundreds of thousands. When evaluating the model one needs only solve a small matrix of size q, therefore the evaluation cost is very low.

$$x = [I-(\tilde{s}_1 M_1+\cdots+\tilde{s}_p M_p)]^{-1} B_M\, u = \sum_{m=0}^{\infty} [\tilde{s}_1 M_1+\cdots+\tilde{s}_p M_p]^m B_M\, u$$
$$= \sum_{m=0}^{\infty} \sum_{k_2=0}^{m-(k_3+\cdots+k_p)} \cdots \sum_{k_{p-1}=0}^{m-k_p} \sum_{k_p=0}^{m} [F^m_{k_2,\ldots,k_p}(M_1,\ldots,M_p) B_M\, u]\ \tilde{s}_1^{m-(k_2+\cdots+k_p)} \tilde{s}_2^{k_2} \ldots \tilde{s}_p^{k_p} \quad (23)$$

$$F^m_{k_2,\ldots,k_p}(M_1,\ldots,M_p) = \begin{cases} 0 & \text{if } k_i \notin \{0,1,\ldots,m\} \quad i=2,\ldots,p \\ 0 & \text{if } k_2+\cdots+k_p \notin \{0,1,\ldots,m\} \\ I & \text{if } m=0 \\ M_1 F^{m-1}_{k_2,\ldots,k_p}(M_1,\ldots,M_p)+M_2 F^{m-1}_{k_2-1,\ldots,k_p}(M_1,\ldots,M_p)+\cdots+M_p F^{m-1}_{k_2,\ldots,k_p-1}(M_1,\ldots,M_p) \end{cases} \quad (24)$$

$$\text{colspan}(V) = \text{span}\{b_M, M_1 b_M, M_2 b_M, \ldots, M_p b_M, M_1^2 b_M, (M_1M_2+M_2M_1)b_M, \ldots \quad (25)$$
$$\ldots, (M_1M_p+M_pM_1)b_M, M_2^2 b_M, (M_2M_3+M_2M_3)b_M, \ldots\},$$
$$= \text{span}\left\{ \bigcup_{m=0}^{m_q} \bigcup_{k_2=0}^{m-(k_p+\cdots+k_3)} \cdots \bigcup_{k_{p-1}=0}^{m-k_p} \bigcup_{k_p=0}^{m} F^m_{k_2,\ldots,k_p}(M_1,\ldots,M_p) b_M \right\}. \quad (26)$$

$$\hat{F}^m_{k_2,\ldots,k_p}\left[-(V^T\tilde{E}_0V)^{-1}V^T\tilde{E}_1V,\ldots,-(V^T\tilde{E}_0V)^{-1}V^T\tilde{E}_pV\right](V^T\tilde{E}_0V)^{-1}V^Tb = V^TF^m_{k_2,\ldots,k_p}[-\tilde{E}_0^{-1}\tilde{E}_1,\ldots,-\tilde{E}_0^{-1}\tilde{E}_p]\tilde{E}_0^{-1}b. \quad (27)$$

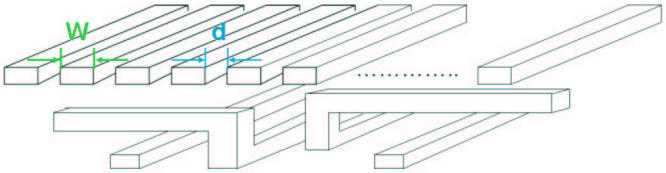

Fig. 4. Sketch of the modeled 16 parallel wires interconnect bus above a random collection of pre-routed interconnect at lower layers.

VII. Example: A bus model parameterized in the wires' spacing

One design consideration for interconnect busses is the trade-off between:

- wider spacing to reduce propagation delays and crosstalk
- narrower spacing to reduce area and therefore cost.

In this example we have used a multi-parameter model order reduction approach to construct a low-order model of an interconnect bus, parameterized by the wire spacing. The model can be efficiently constructed "on the fly" during the design and can account for the topology of the surrounding interconnect already present in the design. Once produced, the model can be simply evaluated for different values of the main parameter, the wire spacing, in order to determine propagation delay, crosstalk or even detailed step responses.

Our example problem is the bus in Fig. 4 which consists of $N = 16$ parallel wires, with thickness $h = 1.2\mu$m, and width $w = 1\mu$m. The total length of each wire is $l = 1$mm. Above and below our bus we assumed a random collection of interconnect at several layout levels ranging from a distance of 1μm to 5μm. We have subdivided each wire into 20 equal sections delimited by $n = 21$ nodes. Each section has been modeled with a resistor. Each node has a "grounded capacitor" representing the interaction with upper and lower interconnect levels. In addition, each node has two coupling capacitors to the adjacent wires on the bus. The value of the capacitors was determined using simple parallel plate formulas. Standard frequency domain nodal analysis leads to a system of equations of the form

$$s\left(C_g+\frac{C_s}{d}\right)v+Gv = Bv_{in} \quad (29)$$
$$v_{out} = Cv,$$

where s is the Laplace Transform variable, d is the spacing between wires, G is the $n\times n$ nodal conductance matrix, The $n\times n$ matrix C_g is the diagonal nodal matrix associated with the grounded capacitors, and C_s is the sparse nodal matrix associated with the adjacent coupling capacitors. B is the $n\times t$ matrix relating t input voltages v_{in} to the n internal node potentials v, C is a $t\times n$ matrix relating node potentials v to the t output voltages v_{out}. We would like to underline that our model is limited to capturing the behavior of the interconnect, which is linear for almost all practical applications. Our models can then be used in conjunction with any device model, from the most simple linear device model to the most sophisticated spice device model. It is not the purpose of this paper to discuss models for devices, however, just in order to "simulate" our interconnect model, for simplicity we will drive our wires with ideal linear devices having impedance $r_d = 1/g_d$. In general when g_d is much smaller than the conductance g of a wire section, all the capacitors in the different sections of each wire appear as lumped, and the detailed model presented here is not necessary. A more interesting case is observed when instead g_d is large. In such

$$\text{colspan}(V) = \text{span}\left\{ \bigcup_{m=0}^{m_q} \bigcup_{k_2=0}^{m-(k_p+\ldots k_3)} \ldots \bigcup_{k_p=0}^{m} F^m_{k_2,\ldots,k_p}(M_1,\ldots,M_p)[b_M]_1, \ldots, \bigcup_{m=0}^{m_q} \bigcup_{k_2=0}^{m-(k_p+\ldots k_3)} \ldots \bigcup_{k_p=0}^{m} F^m_{k_2,\ldots,k_p}(M_1,\ldots,M_p)[b_M]_t \right\} \quad (28)$$

a case, the wires charge up slowly from the input side of the bus and continue to charge up along the length of the bus. In order to observe this more interesting effect we chose $g_d \approx g$. All the wires are left open on the other side.

A. Crosstalk from one input to all outputs

When determining the crosstalk generated on all the outputs by a transition on a single input, the input matrix becomes a vector,

$$B = b = [0 \ldots 0\ g_d\ 0 \ldots 0]^T,$$

and the output matrix is

$$C = \begin{bmatrix} \ldots 010 \ldots & & & \\ & \ldots 010 \ldots & & \\ & & \ddots & \\ & & & \ldots 01 \end{bmatrix}$$

The system in (29) has the following parameterized descriptor matrix

$$E\left(s, \frac{1}{d}\right) = sC_g + s\frac{1}{d}C_s + G;$$

where we choose to work with parameter $1/d$ instead of parameter d. For frequency s we choose as expansion point $\bar{s}_1 = \bar{s} = 0$. For the separation we choose $\bar{s}_2 = 1/d_0 = 1/1\mu$m.

$$E\left(s, \frac{1}{d}\right) = G + s\left[C_g + \frac{1}{d_0}C_s\right] + s\left(\frac{\Delta\left(\frac{1}{d}\right)}{\frac{1}{d_0}}\right)\left[\frac{1}{d_0}C_s\right] \quad (30)$$

Either by identifying terms directly on eq. (30) or by using the formulas in (20)-(21), one can recognize a system as in (19) defining

$$\begin{array}{lllll} \tilde{E}_0 &=& G & & \\ \tilde{E}_1 &=& C_g + \frac{1}{d_0}C_s & \tilde{s}_1 &= s \\ \tilde{E}_2 &=& \frac{1}{d_0}C_s & \tilde{s}_2 &= s\left(\frac{\Delta\left(\frac{1}{d}\right)}{\frac{1}{d_0}}\right) \end{array}$$

The original system for this example has order 336 (16 wires $\times$ 21 nodes each). We performed a model order reduction procedure as described in Section V and obtained a small model capturing the transfer functions from one input to all outputs.

$$\begin{array}{rcl} [\hat{\tilde{E}}_0 + \tilde{s}_1\hat{\tilde{E}}_1 + \tilde{s}_2\hat{\tilde{E}}_2]\hat{x} &=& \hat{b}u \\ y &=& \hat{C}\hat{x}, \end{array} \quad (31)$$

where

$$\begin{array}{rcl} \hat{\tilde{E}}_0 &=& V^T\tilde{E}_0V = V^*GV \\ \hat{\tilde{E}}_1 &=& V^T\tilde{E}_1V = V^T\left[C_g + \frac{1}{d_0}C_s\right]V \\ \hat{\tilde{E}}_2 &=& V^T\tilde{E}_2V = V^T\left[\frac{1}{d_0}C_s\right]V \\ \hat{b} &=& V^Tb \\ \hat{C} &=& CV. \end{array}$$

The projection matrix V can be constructed such that

$$\begin{array}{rcl} \text{colspan}(V) &=& \text{span}\{b_M,\ M_1b_M,\ M_2b_M, \\ && M_1^2b_M,\ (M_1M_2 + M_2M_1)b_M,\ M_2^2b_M,\ \ldots\}, \end{array}$$

where

$$\begin{array}{rcl} b_M &=& \tilde{E}_0^{-1}b = G^{-1}b \\ M_1 &=& -\tilde{E}_0^{-1}\tilde{E}_1 = -G^{-1}\left[C_g + \frac{1}{d_0}C_s\right] \\ M_2 &=& -\tilde{E}_0^{-1}\tilde{E}_2 = -G^{-1}\left[\frac{1}{d_0}C_s\right] \end{array}$$

The Arnoldi algorithm [8] can be used to orthonormalize the columns of V during the matrix construction.

The step response at the end of the wire excited as shown in the top of Fig. 5 is given in the bottom graphs of the same figure. The graphs compare the step responses of the original system (continuous lines) and a reduced model of order three (small crosses) when the spacing distance assumes the values $d = d_0 + \Delta d = 0.5\mu m, 1\mu m, 10\mu$m. The model was constructed using a nominal spacing $d_0 = 1\mu$m, hence the error is smaller near $d \approx d_0 = 1\mu$m. Fig. 5 (below) shows the same comparison with a reduced model of order six. One can notice that the reduced model can be easily and accurately used to evaluate the step response and propagation delay for any value of parameter d near d_0, by plugging into the reduced model (31). From the reduced model (31) we have readily available not only step responses on the same wire, but also crosstalk step responses from one wire to all the other wires. For example, Fig. 6 shows step responses from the input of wire 4 to the output of wires 4, 5, 6 and 7. In this figure we compare again the response of the original system of order 336 (continues curves) with the response of a reduced model order 10 (small crosses) constructed at nominal spacing $d_0 = 1\mu$m, but evaluated in this particular figure at spacing $d = 0.5\mu$m. Note that the model produced by our procedure is parameterized in the wire spacing, hence *any* of such crosstalk responses can be evaluated at *any* spacing. For instance we show in Fig. 7 the response at the output of wire 5 when a step waveform is applied at the input of wire 4 for different spacing values, $d = d_0 + \Delta d = 0.5\mu m, 1\mu m, 10\mu m$.

B. Exploiting the adjoint method for crosstalk from all inputs to one output

It is possible to construct, with the same amount of calculation, a model that provides the susceptibility of one output to all inputs. In order to do this we can use an adjoint method and start from an original system which swaps positions of C and B and transposes all system matrices. Note that since we are considering a single output $C \in \mathbf{R}^{1\times n}$ and $C^T \in \mathbf{R}^{n\times 1}$ is a

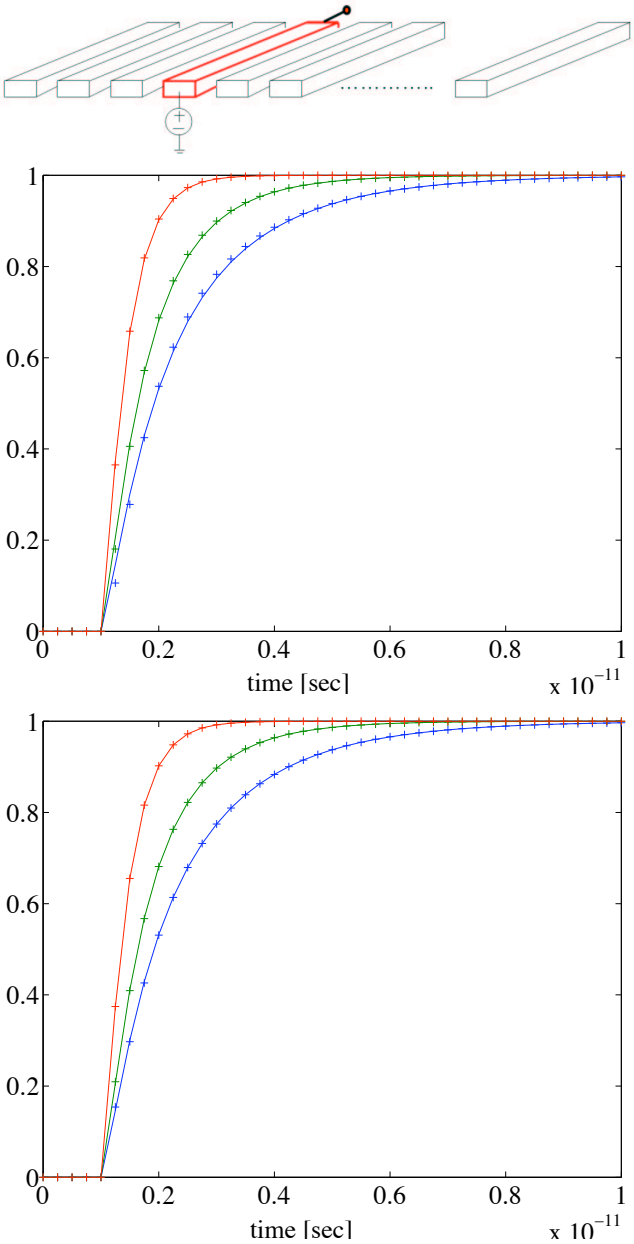

Fig. 5. Responses at the end of wire 4 when a step is applied at the beginning of the same wire. Continuous lines are the response of the original system (order 336). Small crosses are the response of the reduced model, order 3 (top), and order 6 (bottom). The model was constructed using a nominal wire spacing $d_0 = 1um$ and responses are shown here evaluating it at spacings (from the lowest curves to the highest) $d = d_0 + \Delta d = 0.5\mu m, 1\mu m, 10\mu m$.

vector.

$$\begin{aligned} \left[I - (\tilde{s}_1 M_1^T + \tilde{s}_2 M_2^T)\right] v' &= C^T v'_{in} \\ v'_{out} &= B_M^T v', \end{aligned} \tag{32}$$

In this case the columns of the projection operator V will span the Krylov subspace

$$\begin{aligned} \text{colspan}(V') = \text{span}\{ & C^T, M_1^T C^T, M_2^T C^T, M_1^T M_1^T C^T, \\ & (M_1^T M_2^T + M_2^T M_1^T) C^T, M_2^T M_2^T C^T, \ldots\} \end{aligned}$$

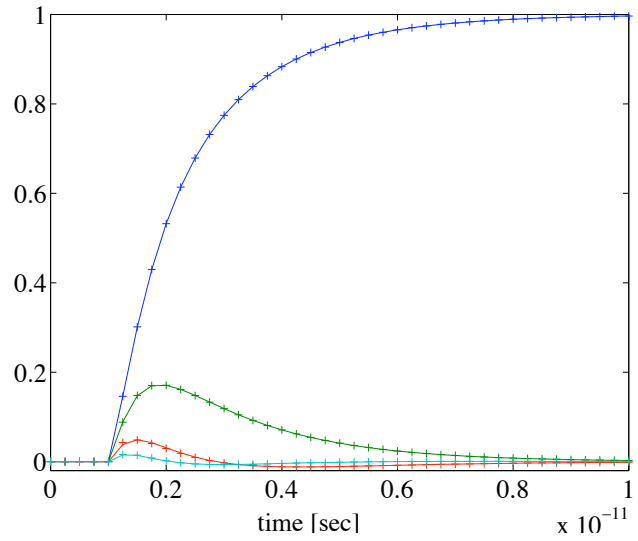

Fig. 6. Responses at the end of wires (from highest to lowest curve) 4, 5, 6 and 7 when a step is applied at the beginning of wire 4. Continuous lines are the response of the original system (order 336). Small crosses are the response of the reduced model (order 10). The model was constructed using a nominal wire spacing $d_0 = 1um$ and responses are shown here evaluating it at spacing $d = 0.5\mu m$.

or in general

$$\text{colspan}(V') = \text{span}\left\{ \bigcup_{m=0}^{m_q} \left(\bigcup_{k=0}^{m} F_k^m(M_1^T, M_2^T) C^T \right) \right\}.$$

In Fig. 8 we show the responses at the end of wire 4 when a step is applied at the beginning of wires 4, 5, 6 and 7. The model was constructed using a nominal wire spacing $d_0 = 1um$. Responses in Fig. 8 (top) are for $d = 0.25\mu m$. Responses in Fig. 8 (bottom) are for $d = 2\mu m$.

VIII. Example: Bus Model Parameterized in Both Wire Width and Separation

Often when designing an interconnect bus, one would like to quickly evaluate design trade-offs originating not only from different wire spacings, but also for different wire widths. Wider wires have lower resistances but use more area and have higher capacitance. The higher capacitance to ground however helps improving crosstalk immunity. We show here a procedure that produces small models that can be easily evaluated with respect to propagation delays and crosstalk performance for different values of the two parameters: wire spacing d, and wire width W. As in the case of wire spacing, we constructed models for a given nominal wire width W_0, and then we parameterized in terms of perturbations ΔW. Considering the same bus example with N parallel wires described in Section VII, we can write the equations for the original large parameterized linear system

$$\begin{aligned} s\left(WC'_g + \frac{C_s}{d}\right) v + WG'v &= Bv_{in} \\ v_{out} &= Cv. \end{aligned}$$

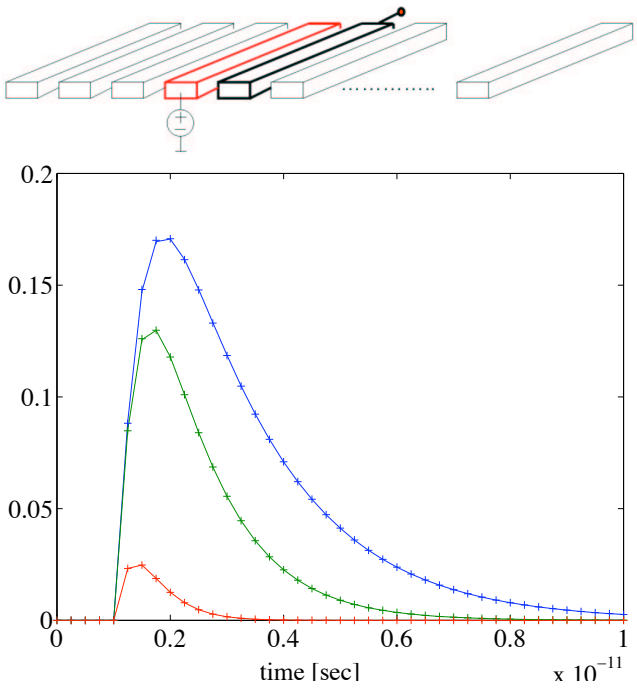

Fig. 7. Crosstalk responses at the end of wire 5 when a step is applied at the beginning of wire 4, for different values of spacing (from highest to lowest curve) $d = d_0 + \Delta d = 0.5\mu m, 1\mu m, 10\mu m$.

The system has the following parameterized descriptor matrix

$$E\left(s, \frac{1}{d}, W\right) = sWC'_g + s\frac{1}{d}C_s + WG';$$

where $C'_g = C_g/W$, $G' = G/W$, and C_g and G are as described in Section VII. With respect to the expansion points $\bar{s}_1 = \bar{s}_0 = 0,\ \bar{s}_2 = 1/d_0,\ \bar{s}_3 = W_0$,

$$\begin{aligned} E\left(s, \frac{1}{d}\right) &= W_0G' + s\left[W_0C'_g + \frac{1}{d_0}C_s\right] + \left(\frac{\Delta W}{W_0}\right)[W_0G'] + \\ &+ s\left(\frac{\Delta W}{W_0}\right)[W_0C'_g] + s\left(\frac{\Delta\left(\frac{1}{d}\right)}{\frac{1}{d_0}}\right)\left[\frac{1}{d_0}C_s\right] \end{aligned} \quad (33)$$

Either by identifying terms directly on eq. (33) or by using the formulas in (20)-(21), one can recognize a system as in (19) defining

$$\begin{array}{llll} \tilde{E}_0 = W_0G' & & \tilde{s}_1 = s & \\ \tilde{E}_1 = W_0C'_g + \frac{1}{d_0}C_s & & \tilde{s}_2 = \frac{\Delta W}{W_0} & \\ \tilde{E}_2 = W_0G' & & \tilde{s}_2 = s\left(\frac{\Delta W}{W_0}\right) & \\ \tilde{E}_3 = W_0C'_g & & \tilde{s}_2 = s\left(\frac{\Delta\left(\frac{1}{d}\right)}{\frac{1}{d_0}}\right) & \\ \tilde{E}_4 = \frac{1}{d_0}C_s & & & \end{array}$$

Following the procedure in Section V the produced reduced order model is

$$\begin{aligned} [\hat{\tilde{E}}_0 + \tilde{s}_1\hat{\tilde{E}}_1 + \tilde{s}_2\hat{\tilde{E}}_2 + \tilde{s}_3\hat{\tilde{E}}_3 + \tilde{s}_4\hat{\tilde{E}}_4]\hat{x} &= \hat{B}u \quad (34) \\ y &= \hat{C}\hat{x}, \end{aligned}$$

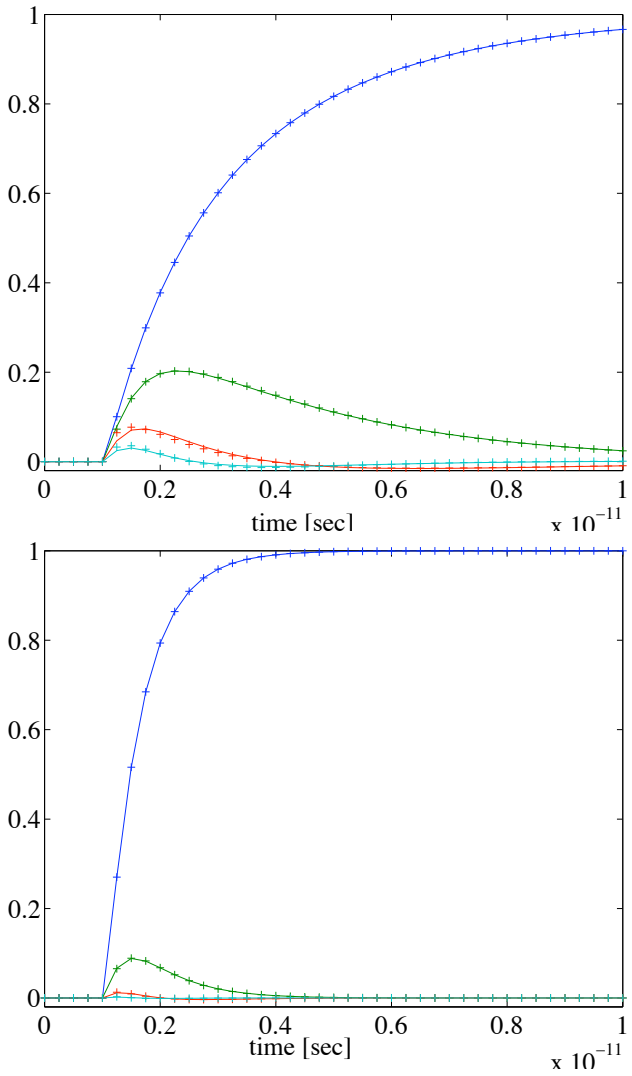

Fig. 8. Adjoint method results: responses at the end of wire 4 when a step is applied at the beginning of wires 4, 5, 6 and 7 (from highest to lowest curve). Continuous lines are the response of the original system (order 336). Small crosses are the response of the reduced model (order 10). The model was constructed using $d_0 = 1um$. The plot on top is for $d = 0.25\mu m$. The plot on the bottom is for $d = 2\mu m$.

where

$$\begin{aligned} \hat{\tilde{E}}_0 &= V^T\tilde{E}_0V = V^*W_0G'V \\ \hat{\tilde{E}}_1 &= V^T\tilde{E}_1V = V^T\left[W_0C'_g + \frac{1}{d_0}C_s\right]V \\ \hat{\tilde{E}}_2 &= V^T\tilde{E}_2V = V^T\left[W_0G'\right]V \\ \hat{\tilde{E}}_3 &= V^T\tilde{E}_3V = V^T\left[W_0C'_g\right]V \\ \hat{\tilde{E}}_4 &= V^T\tilde{E}_4V = V^T\left[\frac{1}{d_0}C_s\right]V \\ \hat{B} &= V^TB \\ \hat{C} &= CV. \end{aligned}$$

The projection matrix V can be constructed for instance for

a single input case ($B = b \in \mathbf{R}^{n\times 1}$) as shown in (26) where

$$\begin{aligned} b_M &= \tilde{E}_0^{-1} b = (W_0 G')^{-1} b \\ M_1 &= -\tilde{E}_0^{-1}\tilde{E}_1 = -(W_0 G')^{-1}\left[W_0 C_g' + \frac{1}{d_0} C_s\right] \\ M_2 &= -\tilde{E}_0^{-1}\tilde{E}_2 = -(W_0 G')^{-1}\left[W_0 G'\right] \\ M_3 &= -\tilde{E}_0^{-1}\tilde{E}_3 = -(W_0 G')^{-1}\left[W_0 C_g'\right] \\ M_4 &= -\tilde{E}_0^{-1}\tilde{E}_4 = -(W_0 G')^{-1}\left[\frac{1}{d_0} C_s\right] \end{aligned}$$

The Arnoldi algorithm [8] can be used to orthonormalize the columns of V during the matrix construction.

In Fig. 9 and 10 we compare the step and crosstalk responses of the original system to the reduced and parameterized model obtained using a Krylov subspace of order $q = 5$. This corresponds to choosing $m_q = 1$ in (26), or in other words it corresponds to constructing a reduced model that matches the original model up to one moment (or derivative) for each parameter s_j. The model was constructed using a nominal spacing $1/d_0 = 1/1\mu$m and nominal wire width $W_0 = 1\mu$m. The key point is that this parameterized model can be rapidly evaluated for any value of spacing and wire width, for instance for a fast and accurate trade-off design optimization procedure.

IX. Conclusions

In this paper we described an approach for generating geometrically - parameterized integrated-circuit interconnect models that are efficient enough for use in interconnect synthesis. The model generation approach presented is automatic, and is based on series expansion of the parameter dependence followed by single or multi-parameter model-reduction. The effectiveness of the techniques described were tested using a multi-line bus example in two different settings. In the first setting, the model reduction approach was used to automatically generate, from an integral equation based capacitance extraction algorithm, second-order models for the dependence of self and coupling capacitances on line separation. In the second setting, multiparameter model reduction was used to generate, from a formula based capacitance and resistance extraction algorithm, high order models for the dependence of delay and cross-talk on line separation and conductor width. The experimental results clearly demonstrated the reduction strategies generated models that were accurate over a wide range of geometric variation.

It should be noted, however, that there are closed-form analytical models which relate geometric parameters to self and coupling capacitances, and the model reduction approaches presented herein are unlikely to be as efficient. However, the methods presented here are potentially more accurate, and certainly more automatic and more flexible. In addition, there are many potential issues that can lead to new contributions in this field. The multi-parameter method was tested using only resistor-capacitor interconnect models, and accuracy issues may arise when inductance is included. We also did not investigate using multi-point moment-matching, which could be a better choice given the range of the parameters is often known a-priori. In addition, the multi-parameter reduction method can become quite expensive when a large accuracy is required and the model has a large number of parameters, so the method would not generate a very efficient model if each wire pair spacing in a 16 wire bus was treated individually. Finally, there are some interesting error bounds in [4], and these results could be applied to automatically select the reduction order.

X. Acknowledgments

The authors would like to thank Jung Hoon Lee, Xin Hu and David Willis for correcting many typos while reviewing a pre-print version of this article, and the prototype Matlab code for this work.

This work was in part supported by the Singapore-MIT Alliance, the Semiconductor Research Corporation, and the DARPA NeoCAD program managed by the Sensors Directorate of the Air Force Laboratory, USAF, Wright-Patterson AFB.

Appendix

A. Proof of Lemma 1

Lemma 1 can be shown by induction on m. For $m = 0$ we can easily verify that

$$[\tilde{s}_1 M_1 + \cdots + \tilde{s}_p M_p]^0 = I.$$

Let us now assume for $m-1$ that (35) holds. In order to show that the property holds for m we can first write (36). Multiplying and collecting the terms with the same powers of $\tilde{s}_1, \ldots, \tilde{s}_p$ we obtain (37), which proves that the statement holds for m.

B. Proof of Lemma 2

As from [8], if $z \in \text{colspan}(V)$ then there must exist a vector y such that $Vy = z$. Substituting $VV^T z = VV^T Vy = Vy = z$.

C. Proof of Lemma 3

As from [8], we need to show that $y = V^T \tilde{E}_0^{-1} z$ is a solution for the linear system $(V^T \tilde{E}_0 V)y = V^T z$. Substituting, $(V^T \tilde{E}_0 V)y = (V^T \tilde{E}_0 V)V^T \tilde{E}_0^{-1} z$. Since $\tilde{E}_0^{-1} z \in \text{colspan}(V)$ from Lemma 2 we have that $V^T \tilde{E}_0 VV^T \tilde{E}_0^{-1} z = V^T \tilde{E}_0 \tilde{E}_0^{-1} z = V^T z$.

D. Proof of Lemma 4

A proof is given in this paper by induction on the order m of the coefficient. First let us prove the statement in the lemma for $m = 0$, i.e.

$$\begin{aligned} \hat{F}^0_{k_2,\ldots,k_p}\left[-(V^T\tilde{E}_0V)^{-1}V^T\tilde{E}_1V, \ldots, -(V^T\tilde{E}_0V)^{-1}V^T\tilde{E}_pV\right] \cdot \\ \cdot (V^T\tilde{E}_0V)^{-1}V^Tb \\ = I(V^T\tilde{E}_0V)^{-1}V^Tb. \end{aligned}$$

Since $\tilde{E}_0^{-1} b \in \text{colspan}(V)$, from Lemma 3 we have

$$\begin{aligned} (V^T\tilde{E}_0V)^{-1}V^Tb &= V^T\tilde{E}_0^{-1}b \\ &= V^T F^0_{k_2,\ldots,k_p}[-\tilde{E}_0^{-1}\tilde{E}_1, \ldots, -\tilde{E}_0^{-1}\tilde{E}_p]\tilde{E}_0^{-1}b. \end{aligned}$$

$$\left[\tilde{s}_1 M_1 + \cdots + \tilde{s}_p M_p\right]^{m-1} = \sum_{k_2=0}^{(m-1)-(k_3+\cdots+k_p)} \cdots \sum_{k_{p-1}=0}^{(m-1)-k_p} \sum_{k_p=0}^{m-1} \left\{ \left[F^{m-1}_{k_2,\ldots,k_p}(M_1,\ldots,M_p)\right] \quad \tilde{s}_1^{(m-1)-(k_2+\cdots+k_p)} \tilde{s}_2^{k_2} \ldots \tilde{s}_p^{k_p} \right\}. \tag{35}$$

$$\begin{aligned}
&\left[\tilde{s}_1 M_1 + \cdots + \tilde{s}_p M_p\right]^{m} = \\
&= \left[\tilde{s}_1 M_1 + \cdots + \tilde{s}_p M_p\right] \sum_{k_2=0}^{(m-1)-(k_3+\cdots+k_p)} \cdots \sum_{k_{p-1}=0}^{(m-1)-k_p} \sum_{k_p=0}^{m-1} \left\{ \left[F^{m-1}_{k_2,\ldots,k_p}(M_1,\ldots,M_p)\right] \quad \tilde{s}_1^{(m-1)-(k_2+\cdots+k_p)} \tilde{s}_2^{k_2} \ldots \tilde{s}_p^{k_p} \right\} \qquad (36)\\
&= \sum_{k_2=0}^{(m-1)-(k_3+\cdots+k_p)} \cdots \sum_{k_{p-1}=0}^{(m-1)-k_p} \sum_{k_p=0}^{m-1} \left\{ \tilde{s}_1 M_1 F^{m-1}_{k_2,\ldots,k_p}(M_1,\ldots,M_p) \ \tilde{s}_1^{(m-1)-(k_2+\cdots+k_p)} \tilde{s}_2^{k_2} \ldots \tilde{s}_p^{k_p} + \ldots \right.\\
&\qquad \left. \cdots + \tilde{s}_p M_p F^{m-1}_{k_2,\ldots,k_p-1}(M_1,\ldots,M_p) \ \tilde{s}_1^{m-(k_2+\cdots+k_p)} \tilde{s}_2^{k_2} \ldots \tilde{s}_p^{k_p-1} \right\}\\
&= \sum_{k_2=0}^{(m-1)-(k_3+\cdots+k_p)} \cdots \sum_{k_{p-1}=0}^{(m-1)-k_p} \sum_{k_p=0}^{m-1} \left\{ \left[M_1 F^{m-1}_{k_2,\ldots,k_p}(M_1,\ldots,M_p) + \cdots + M_p F^{m-1}_{k_2,\ldots,k_p-1}(M_1,\ldots,M_p)\right] \tilde{s}_1^{m-(k_2+\cdots+k_p)} \tilde{s}_2^{k_2} \ldots \tilde{s}_p^{k_p} \right\} \qquad (37)
\end{aligned}$$

$$\begin{aligned}
&\hat{F}^m_{k_2,\ldots,k_p}\left[-(V^T\tilde{E}_0V)^{-1}V^T\tilde{E}_1V,\ldots,-(V^T\tilde{E}_0V)^{-1}V^T\tilde{E}_pV\right] \ (V^T\tilde{E}_0V)^{-1}V^Tb = \qquad (38)\\
&= \left[(V^T\tilde{E}_0V)^{-1}V^T\tilde{E}_1V\hat{F}^{m-1}_{k_2,\ldots,k_p}(-(V^T\tilde{E}_0V)^{-1}V^T\tilde{E}_1V,\ldots,-(V^T\tilde{E}_0V)^{-1}V^T\tilde{E}_pV) + \ldots \right.\\
&\qquad \left. \cdots + (V^T\tilde{E}_0V)^{-1}V^T\tilde{E}_pV\hat{F}^{m-1}_{k_2,\ldots,k_p-1}(-(V^T\tilde{E}_0V)^{-1}V^T\tilde{E}_1V,\ldots,-(V^T\tilde{E}_0V)^{-1}V^T\tilde{E}_pV) \right] \ (V^T\tilde{E}_0V)^{-1}V^Tb\\
&= \left[(V^T\tilde{E}_0V)^{-1}V^T\tilde{E}_1VV^TF^{m-1}_{k_2,\ldots,k_p}(-\tilde{E}_0^{-1}\tilde{E}_1,\ldots,-\tilde{E}_0^{-1}\tilde{E}_p) + \cdots + (V^T\tilde{E}_0V)^{-1}V^T\tilde{E}_pVV^TF^{m-1}_{k_2,\ldots,k_p-1}(-\tilde{E}_0^{-1}\tilde{E}_1,\ldots,-\tilde{E}_0^{-1}\tilde{E}_p)\right]\tilde{E}_0^{-1}b \qquad (39)\\
&= \left[(V^T\tilde{E}_0V)^{-1}V^T\tilde{E}_1F^{m-1}_{k_2,\ldots,k_p}(-\tilde{E}_0^{-1}\tilde{E}_1,\ldots,-\tilde{E}_0^{-1}\tilde{E}_p) + \cdots + (V^T\tilde{E}_0V)^{-1}V^T\tilde{E}_pF^{m-1}_{k_2,\ldots,k_p-1}(-\tilde{E}_0^{-1}\tilde{E}_1,\ldots,-\tilde{E}_0^{-1}\tilde{E}_p)\right] \ \tilde{E}_0^{-1}b\\
&= (V^T\tilde{E}_0V)^{-1}V^T\left[\tilde{E}_1F^{m-1}_{k_2,\ldots,k_p}(-\tilde{E}_0^{-1}\tilde{E}_1,\ldots,-\tilde{E}_0^{-1}\tilde{E}_p) + \cdots + \tilde{E}_pF^{m-1}_{k_2,\ldots,k_p-1}(-\tilde{E}_0^{-1}\tilde{E}_1,\ldots,-\tilde{E}_0^{-1}\tilde{E}_p)\right]\tilde{E}_0^{-1}b \qquad (40)\\
&= V^TF^m_{k_2,\ldots,k_p}\left[-\tilde{E}_0^{-1}\tilde{E}_1,\ldots,-\tilde{E}_0^{-1}\tilde{E}_p\right] \ \tilde{E}_0^{-1}b. \qquad (41)
\end{aligned}$$

This concludes the proof for m=0. Let us now assume that the statement is correct for order $m-1$ and let us show that this implies it is correct for order m. From the recursive definition formula (24), we have (38), Using the inductive hypothesis on order $m-1$ for each of the terms in the summation we have (39). Using Lemma 2 on each of the terms of the summation we have (40). Since

$$\begin{aligned}
&\tilde{E}_0^{-1}\left[\tilde{E}_1F^{m-1}_{k_2,\ldots,k_p}(\tilde{E}_0^{-1}\tilde{E}_1,\ldots,\tilde{E}_0^{-1}\tilde{E}_p) + \ldots \right.\\
&\left. \cdots + \tilde{E}_pF^{m-1}_{k_2,\ldots,k_p-1}(\tilde{E}_0^{-1}\tilde{E}_1,\ldots,\tilde{E}_0^{-1}\tilde{E}_p)\right]\tilde{E}_0^{-1}b \quad =\\
&\qquad = F^m_{k_2,\ldots,k_p}[\tilde{E}_0^{-1}\tilde{E}_1,\ldots,\tilde{E}_0^{-1}\tilde{E}_p]\tilde{E}_0^{-1}b \quad =\\
&\qquad\quad = F^m_{k_2,\ldots,k_p}[\tilde{E}_0^{-1}\tilde{E}_1,\ldots,\tilde{E}_0^{-1}\tilde{E}_p]b_M \quad \in \quad \text{colspan}(V)
\end{aligned}$$

we can use Lemma 3 and obtain (41). Note that the hypothesis for Lemma 2 and Lemma 3 in this context hold only for $m = 0,1,\ldots,m_q$, hence (27) holds only for $m = 0,1,\ldots,m_q$. This concludes the proof of Lemma 4.

E. Proof of Theorem 1

The transfer function of the system in (19) for a single input case ($B = b \in \mathbf{R}^{n\times 1}$) is given by (42). Similarly the transfer function of the system in (22) is given by (43). Using first Lemma 4, and then Lemma 2, we can see that each moment of the reduced model transfer function expansion (43) matches the corresponding moment of the original transfer function expansion (42)

$$\begin{aligned}
C\hat{F}^m_{k_2,\ldots,k_p}[-(V^T\tilde{E}_0V)^{-1}V^T\tilde{E}_1V,\ldots,-(V^T\tilde{E}_0V)^{-1}V^T\tilde{E}_pV]&\\
(V^T\tilde{E}_0V)^{-1}V^Tb \quad &=\\
CVV^TF^m_{k_2,\ldots,k_p}(-\tilde{E}_0^{-1}\tilde{E}_1,\ldots,-\tilde{E}_0^{-1}\tilde{E}_p)\tilde{E}_0^{-1}b \quad &=\\
CF^m_{k_2,\ldots,k_p}(-\tilde{E}_0^{-1}\tilde{E}_1,\ldots,-\tilde{E}_0^{-1}\tilde{E}_p)\tilde{E}_0^{-1}b \quad &=\\
CF^m_{k_2,\ldots,k_p}(-\tilde{E}_0^{-1}\tilde{E}_1,\ldots,-\tilde{E}_0^{-1}\tilde{E}_p)b_M.&
\end{aligned}$$

Note that Lemma 2 and Lemma 3 in this context hold only for the first q moments corresponding to $m = 0,1,\ldots,m_q$, hence only those moments are guaranteed to be matched.

F. Proof of Lemma 5

The number $f_{m,p}$ of coefficients of order m, for a system with p parameters, can be obtained by induction

$$f_{m,p} = \begin{cases} 1 & \text{if } m = 0, \\ \sum_{k=1}^{p} f_{m-1,k} & \text{if } m > 0 \end{cases}$$

or equivalently,

$$\begin{aligned}
f_{m,p} \quad &= \quad \binom{m+p-1}{m} = \binom{m+p-1}{p-1} = f_{p-1,m+1}\\
&= \quad \frac{(m+p-1)!}{m!(p-1)!}
\end{aligned}$$

$$H = C\left[I-(\tilde{s}_1M_1+\cdots+\tilde{s}_pM_p)\right]^{-1}\ \tilde{E}_0^{-1}b \tag{42}$$
$$= \sum_{m=0}^{\infty}\sum_{k_2=0}^{m-(k_3+\cdots+k_p)}\cdots\sum_{k_{p-1}=0}^{m-k_p}\sum_{k_p=0}^{m}\left\{\left[CF^m_{k_2,\ldots,k_p}(M_1,\ldots,M_p)b_M\right]\ \tilde{s}_1^{m-(k_2+\cdots+k_p)}\tilde{s}_2^{k_2}\ldots\tilde{s}_p^{k_p}\right\}.$$

$$\hat{H} = CV\left\{I-\left[\tilde{s}_1(V^T(-\tilde{E}_0)V)^{-1}V^T\tilde{E}_1V+\cdots+\tilde{s}_p(V^T(-\tilde{E}_0)V)^{-1}V^T\tilde{E}_pV\right]\right\}^{-1}\ (V^T\tilde{E}_0V)^{-1}V^Tb \tag{43}$$
$$= \sum_{m=0}^{\infty}\sum_{k_2=0}^{m-(k_3+\cdots+k_p)}\cdots\sum_{k_{p-1}=0}^{m-k_p}\sum_{k_p=0}^{m}\left\{\left[CV\hat{F}^m_{k_2,\ldots,k_p}\left(-(V^T\tilde{E}_0V)^{-1}V^T\tilde{E}_1V,\ldots,-(V^T\tilde{E}_0V)^{-1}V^T\tilde{E}_pV\right)(V^T\tilde{E}_0V)^{-1}V^Tb\right]\tilde{s}_1^{m-(k_2+\cdots+k_p)}\tilde{s}_2^{k_2}\ldots\tilde{s}_p^{k_p}\right\}$$

Using then the asymptotic approximation [21] for the Gamma Function $\Gamma(z)=(z-1)!$, one obtains

$$f_{m,p}=\frac{\Gamma(m+p)}{\Gamma(m+1)\Gamma(p)}\approx\frac{e}{\sqrt{2\pi}}\frac{(m+p)^{m+p-\frac{1}{2}}}{m^{m+\frac{1}{2}}p^{p-\frac{1}{2}}}.$$

Observing that for most practical problems $m<<p$, we have

$$f_{m,p}=O\left(\frac{p^m}{m^{m+\frac{1}{2}}}\right).$$

The order q of the produced parameterized reduced system is then

$$q=\sum_{m=0}^{m_q}f_{m,p}=O(m_qf_{m,q})=O\left(\frac{p^{m_q}}{m_q^{m_q-\frac{1}{2}}}\right).$$

REFERENCES

[1] Y Liu, Lawrence T. Pileggi, and Andrzej J. Strojwas. Model order-reduction of RCL interconnect including variational analysis. In *Proc. of the ACM/IEEE Design Automation Conference*, pages 201–206, New Orleans, Louisiana, June 1999.

[2] P. Heydari and M. Pedram. Model reduction of variable-geometry interconnects using variational spectrally-weighted balanced truncation. In *Proc. of IEEE/ACM International Conference on Computer Aided-Design*, San Jose, CA, November 2001.

[3] S. Pullela, N. Menezes, and L.T. Pileggi. Moment-sensitivity-based wire sizing for skew reduction in on-chip clock nets. *IEEE Trans. Computer-Aided Design*, 16(2):210–215, February 1997.

[4] C. Prud'homme, D. Rovas, K. Veroy, Y. Maday, A.T. Patera, and G. Turinici. Reliable real-time solution of parametrized partial differential equations: Reduced-basis output bounds methods. *Journal of Fluids Engineering*, 2002.

[5] K. Gallivan, E. Grimme, and P. Van Dooren. Asymptotic Waveform Evaluation via a Lanczos Method. *Applied Mathematics Letters*, 7(5):75–80, 1994.

[6] Peter Feldmann and Roland W. Freund. Reduced-order modeling of large linear subcircuits via a block Lanczos algorithm. In 32^{nd} *ACM/IEEE Design Automation Conference*, pages 474–479, San Francisco, CA, June 1995.

[7] K. J. Kerns, I. L. Wemple, and A. T. Yang. Stable and efficient reduction of substrate model networks using congruence transforms. In *Proc. of IEEE/ACM International Conference on Computer Aided-Design*, pages 207 – 214, San Jose, CA, November 1995.

[8] Eric Grimme. *Krylov Projection Methods for Model Reduction*. PhD thesis, Coordinated-Science Laboratory, University of Illinois at Urbana-Champaign, Urbana-Champaign, IL, 1997.

[9] I. M. Elfadel and D. D. Ling. A block Arnoldi algorithm for multipoint passive model-order reduction of multiport RLC networks. *Proc. of IEEE/ACM International Conference on Computer Aided-Design*, November 1997.

[10] A. Odabasioglu, M. Celik, and L. T. Pileggi. PRIMA: passive reduced-order interconnect macromodeling algorithm. *IEEE Trans. Computer-Aided Design*, 17(8):645–654, August 1998.

[11] L. M. Silveira, M. Kamon, I. Elfadel, and J. White. Coordinate-transformed Arnoldi algorithm for generating guarantee stable reduced-order models of RLC. *Computer Methods in Applied Mechanics and Engineering*, 169(3-4):377–89, February 1999.

[12] J. E. Bracken, D. K. Sun, and Z. Cendes. Characterization of electromagnetic devices via reduced-order models. *Computer Methods in Applied Mechanics and Engineering*, 169(3-4):311–330, February 1999.

[13] A. C. Cangellaris and L. Zhao. Passive reduced-order modeling of electromagnetic systems. *Computer Methods in Applied Mechanics and Engineering*, 169(3-4):345–358, February 1999.

[14] D. S. Weile, E. Michielssen, Eric Grimme, and K. Gallivan. A method for generating rational interpolant reduced order models of two-parameter linear systems. *Applied Mathematics Letters*, 12:93–102, 1999.

[15] J. R. Phillips, E. Chiprout, and D. D. Ling. Efficient full-wave electromagnetic analysis via model-order reduction of fast integral transforms. In 33^{rd} *ACM/IEEE Design Automation Conference*, pages 377–382, Las Vegas, Nevada, June 1996.

[16] K. Nabors and J. White. FastCap: a multipole accelerated 3-d capacitance extraction program. *IEEE Trans. on Computer-Aided Design of Integrated Circuits and Systems*, 10(11):1447–59, November 1991.

[17] M. Kamon, M. J. Tsuk, and J. K. White. FASTHENRY: A multipole-accelerated 3-D inductance extraction program. *IEEE Trans. on Microwave Theory and Techniques*, 42(9):1750–8, September 1994.

[18] J. R. Phillips and J. White. A Precorrected-FFT method for electrostatic analysis of complicated 3-D structures. *IEEE Trans. on Computer-Aided Design of Integrated Circuits and Systems*, 16(10):1059–1072, October 1997.

[19] J. Tausch and J. White. A multiscale method for fast capacitance extraction. In *Proc. of the IEEE/ACM Design Automation Conference*, pages 537–42, New Orleans, LA, June 1999.

[20] S. Kapur and D. Long. Large scale capacitance calculations. In *Proc. of the IEEE/ACM Design Automation Conference*, pages 744–9, Los Angeles, June 2000.

[21] M. Abramowitz and I. A. Stegun. *Handbook of mathematical functions with formulas, graphs, and mathematical tables*. Washington: U.S. Govt. Print. Off., 1972.

Luca Daniel (S'98) is currently an Assistant Professor in Electrical Engineering and Computer Science at the Massachusetts Institute of Technology (MIT). He received the Laurea degree summa cum laude in Electronic Engineering from "Universita' di Padova", Italy in 1996, and the Ph.D. degree in Electrical Engineering and Computer Science from Univ. of California, Berkeley, in 2003. His PhD thesis received the Sakrison Memorial Prize from the Dept. of Electrical Engineering and Computer Science at UC Berkeley, and the Friedman Memorial Prize in Applied Mathematics, from the Dept. of Mathematics at UC Berkeley. Luca also received four best paper awards in conferences, and the "IEEE Power Electronic Society Prize Paper Award" for the best paper published on IEEE Trans. on Power Electronics in the year 1999. In addition to these academic activities, Luca has worked in 1998 at the Hewlett-Packard Labs in Palo Alto, CA, and in 2001 at the Cadence Berkeley Labs, Berkeley, CA. His research interests include model order reduction, parasitic extraction, electromagnetic interference, mixed- signal and RF circuit design, power electronics, MEMs design and modeling.

Ong, Chin Siong received his B.Eng degree in Electrical Engineering from National University of Singapore (NUS) in 2000, and his M.Eng in High Performance Computing in Engineered Systems from Singapore MIT Alliance from NUS in 2002. He is currently working as an Engineer developing Virtual Private Network in Digisafe Pte Ltd.

Low Sok Chay received her B.S. degree in computational science and mathematics and her M.Eng. in High Performance Computation in Engineered Systems from National University of Singapore in year 2000 and 2002 respectively. She is currently working as an operations analyst in the Defense Science and Technology Agency in Singapore.

Kwok Hong Lee, a valued colleague, passed away before publication of this paper. He was an active researcher in computational mechanics, a vice-dean of engineering and an associate professor in mechanical engineering at the National University of Singapore

Jacob White (S'80-M'83) received his B.S. degree in electrical engineering and computer science from the Massachusetts Institute of Technology and his S.M. and Ph. D. degree in electrical engineering and computer science from the University of California, Berkeley. He worked at the IBM T. J. Watson research center from 1985 to 1987, was the Analog Devices Career Development Assistant Professor at the Massachusetts Institute of Technology from 1987 to 1989, was a 1988 Presidential Young Investigator, and was an associate editor of the IEEE Transactions on Computer-Aided Design from 1992 until 1996, and was chair of the International Conference on Computer-Aided Design in 1999. Jacob White is currently at the Massachusetts Institute of Technology where he is a professor in Electrical Engineering and Computer Science and an associate director of the Research Laboratory of Electronics. His current research interests are in numerical algorithms for problems in circuits, interconnect, micromachined devices and biological systems.

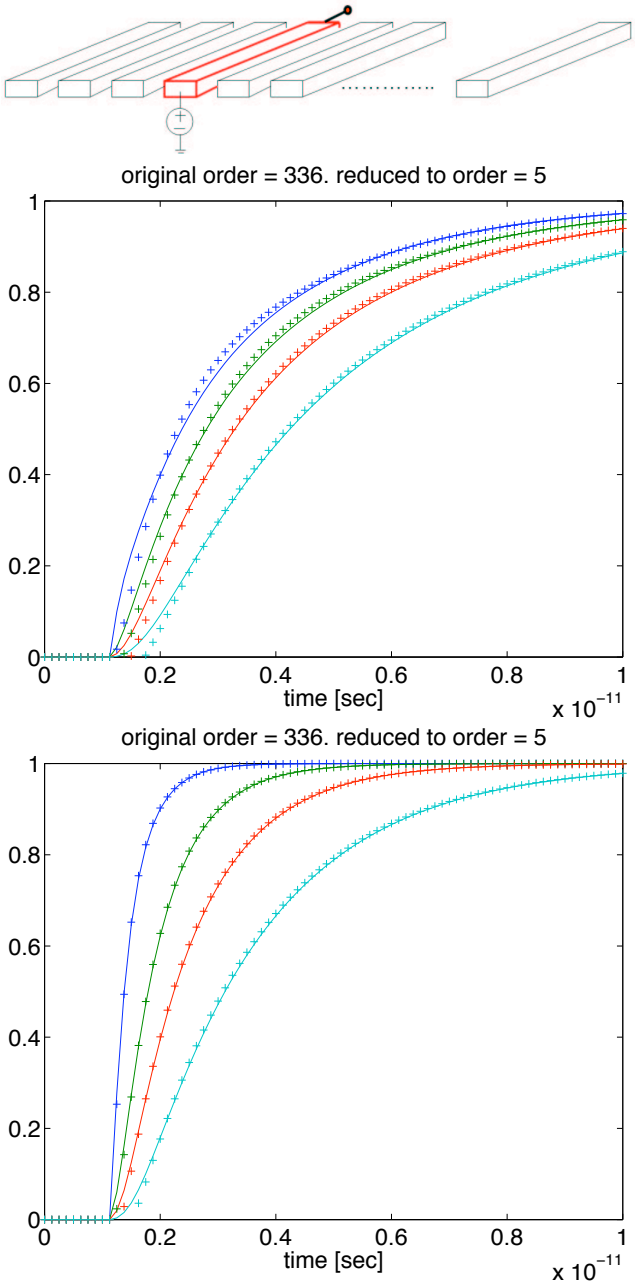

Fig. 9. Original system (continuous curves) versus 5^{th} order reduced model (small crosses) using both spacing and width parameters. The nominal wire spacing was $d_0 = 1\mu$m and the nominal wire width was $W = 1\mu$m. Top: responses at the end of wire 4 due to a step at the beginning of the same wire for different widths (from highest to lowest curve) $W = .25\mu\text{m}, 2\mu\text{m}, 4\mu\text{m}, 8\mu\text{m}$ and for spacing $d = .25\mu$m. Bottom: same responses but for spacing $d = 2\mu$m.

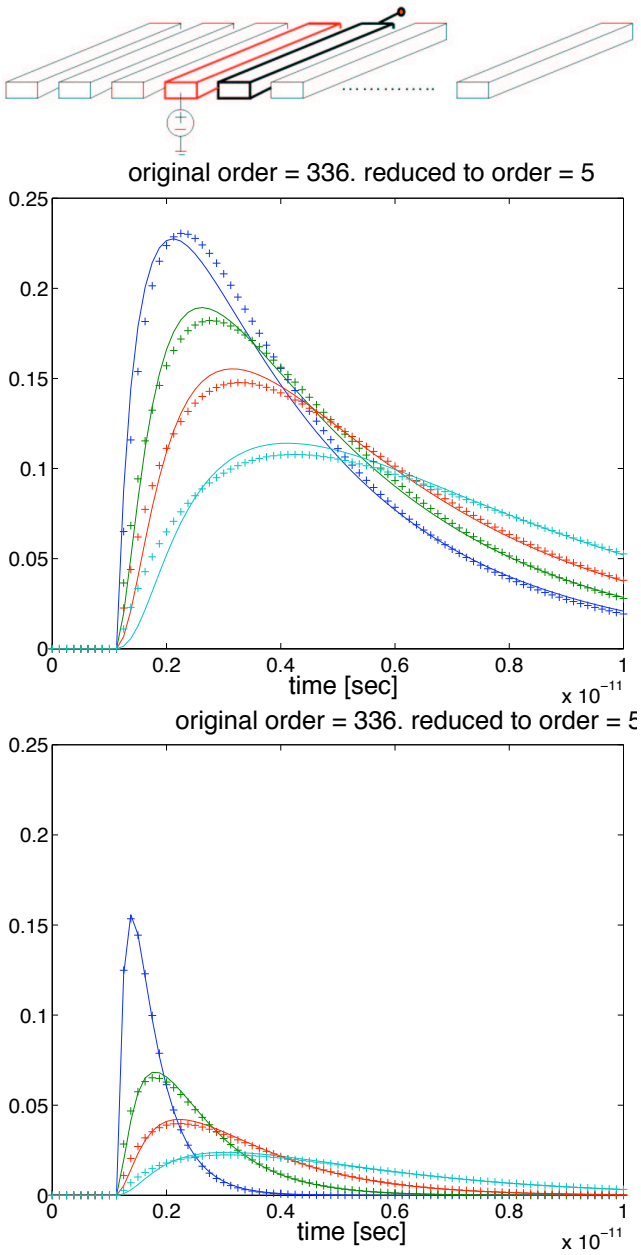

Fig. 10. Original system (continuous curves) versus 5^{th} order reduced model (small crosses) using both spacing and width parameters. The nominal wire spacing was $d_0 = 1\mu$m and the nominal wire width was $W = 1\mu$m. Top: crosstalk at the end of wire 5 due to a step at the beginning of wire 4. Curves correspond to widths (from highest curve to lowest) $W = .25\mu\text{m}, 2\mu\text{m}, 4\mu\text{m}, 8\mu\text{m}$ and spacing is $d = .25\mu$m. Bottom: same crosstalk responses but for spacing $d = 2\mu$m.